TU Delft

Delft University of Technology

Document Version
Final published version

Citation (APA)
Feijen, P., Mirra, G., & Overend, M. (2026). A Computational Design-to-Fabrication Workflow for Freeform Deployable Structures Using Auxetic Lattice Mechanisms. In A. Manuello Bertetto, S. Gabriele, F. Marmo, & A. Micheletti (Eds.), *Proceedings of IASS-IWSS 2026 : R-Evolution of Shapes: Sustainability, Re-Use, and new Design Paradigms* IASS.

Important note
To cite this publication, please use the final published version (if applicable).
Please check the document version above.

Copyright
In case the licence states “Dutch Copyright Act (Article 25fa)”, this publication was made available Green Open Access via the TU Delft Institutional Repository pursuant to Dutch Copyright Act (Article 25fa, the Taverne amendment). This provision does not affect copyright ownership.
Unless copyright is transferred by contract or statute, it remains with the copyright holder.

Sharing and reuse
Other than for strictly personal use, it is not permitted to download, forward or distribute the text or part of it, without the consent of the author(s) and/or copyright holder(s), unless the work is under an open content license such as Creative Commons.

Takedown policy
Please contact us and provide details if you believe this document breaches copyrights.
We will remove access to the work immediately and investigate your claim.

This work is downloaded from Delft University of Technology.

Proceedings of IASS-IWSS 2026 — September 14-18, 2026, Turin, Italy
"R-Evolution of Shapes: Sustainability, Re-Use, and New Design Paradigms"
Annual Symposium of the International Association for Shell and Spatial Structures
3rd Italian Workshop on Shel and Spatial Structures
A. Manuello Bertetto, S. Gabriele, F. Marmo, A. Micheletti (eds.)

A Computational Design-to-Fabrication Workflow for Freeform Deployable Structures Using Auxetic Lattice Mechanisms

Pepijn FEIJEN*, Gabriele MIRRA, Mauro OVEREND

Department of Architectural Engineering and Technology, Delft University of Technology
Julianalaan 134, 2628 BL Delft, The Netherlands
pepijnfeijen@gmail.com

Abstract

Deployable structures offer advantages in logistics and adaptability, but they must satisfy tightly interconnected geometric, kinematic, and structural constraints across both undeployed and deployed configurations. This increases modelling complexity and often requires complex mechanical assemblies, limiting broader architectural applicability. Recent research on mechanical metamaterials has demonstrated how global structural behavior can be programmed through local material organization, enabling controlled deformation without conventional hinges or joints. When combined with large-scale additive manufacturing, these metamaterials offer new possibilities for deployable architectural systems that can be fabricated flat and erected through deployment.

This paper presents a computational design-to-fabrication workflow for modelling, simulating, and prototyping freeform deployable structures based on auxetic lattice mechanisms. The proposed system consists of a layered rotating auxetic lattice that transforms from an initially flat configuration into a doubly curved shell geometry. A form-finding method based on dynamic relaxation establishes a relationship between flat and deployed states while ensuring kinematic compatibility.

The workflow is tested across multiple target geometries and evaluated through numerical simulations and 3D-printed prototypes at different scales. The results demonstrate the potential of the proposed system for architectural applications, while also highlighting the opportunities and challenges associated with the fabrication, deployment, and scaling of auxetic lattice-based deployable structures.

Keywords: Deployable structures, auxetic lattices, mechanical metamaterials, form-finding, inverse design, computational design, large-scale additive manufacturing, programmable materials

1. Introduction

Deployable structures are engineered systems designed to transform from a compact configuration into a larger operational form. Their ability to significantly reduce transport volume and simplify on-site assembly makes them attractive for applications such as temporary shelters, space structures, retractable roofs, and portable infrastructure [1,2]. Nevertheless, designing these systems requires resolving tightly interconnected kinematic and structural constraints to preserve the compatibility between undeployed and deployed states. This remains a significant computational challenge, especially for non-standard systems, such as free-form shell structures. Furthermore, deployable structures often rely on complex mechanical assemblies such as hinges, scissor mechanisms, or articulated joints to realize the kinematic behavior, increasing both production and maintenance costs. Recent advances in additive manufacturing have enabled the fabrication of geometries with embedded kinematic behavior, reducing reliance on complex mechanical assemblies and combining structural and mechanical functions within a single system [3,4]. The proposed system operates between two interdependent states: a flat production state and a deployed spatial state. The production state prioritizes fabrication efficiency and compactness,

Copyright © 2026 by Pepijn Feijen, Gabriele Mirra, Mauro Overend
Published by the International Association for Shell and Spatial Structures (IASS) with permission.

while the deployed state focuses on structural performance and geometric approximation of a target surface. A computational form-finding workflow is developed to simulate deployment and refine the design while preserving kinematic compatibility between both states throughout the process. While recent studies have explored 3D-printed mechanical metamaterials, their application to architectural-scale components remains limited. This paper contributes to this area by presenting the development of physical prototypes and full-scale mock-ups that address constraints related to the fabrication process, material behavior, and structural performance.

The paper is structured as follows. Section 2 reviews relevant work on deployable structures, mechanical metamaterials, inverse design, and additive manufacturing. Section 3 introduces the proposed computational workflow, including the kinematic system and dual-state design logic. Section 4 presents the form-finding methodology, including the constraint system and validation across different target geometries. Section 5 describes materialization, structural analysis, and parametric optimization through a design application at the architectural scale. Section 6 presents prototyping and fabrication studies used to evaluate material behavior and manufacturing constraints. Section 7 discusses the results, limitations, and future work, followed by the conclusions in Section 8.

2. Background

The design of deployable structures for additive manufacturing has increasingly integrated mechanical metamaterial principles, whereby global mechanical behavior is primarily determined by the geometry and arrangement of internal structures rather than by the base material itself [5]. By arranging repeating units with controlled connectivity and constraints, deformation modes such as expansion, contraction, bending, or twisting can be embedded into the material system [3]. Panetta et al. [6] distinguish two primary approaches for designing kinematic systems such as deployable structures and mechanical metamaterials: forward design and inverse design. The forward design approach starts from a known initial configuration and simulates its transformation to predict the deployed shape, which is often an iterative and time-consuming process [6]. In contrast, the inverse design method starts with a target (deployed) geometry and searches for the initial undeployed configuration that best approximates the target geometry after deployment. This approach has been implemented through digital form-finding methods [7]. Other studies on deployable systems have focused on the material scale, with explorations in additive manufacturing. Studies by Ou et al. [3] and Ion et al. [4] demonstrate how assemblies of rigid elements and compliant hinges can be effectively designed for additive manufacturing. Ou et al. [3] present small-scale 3D-printed transformable planar assemblies based on rotational mechanisms, where coordinated element rotation enables controlled expansion. Similarly, Pan et al. [8] developed kirigami-based metamaterials in which patterned cuts allow flat sheets to deploy into doubly curved surfaces through localized bending and rotation. Both studies primarily adopt a forward design approach, using parametric modelling to automate the generation and analysis of various structural configurations. Complementary research on additive manufacturing by Chen et al. [7] and Konaković et al. [9,10] focused instead on inverse design methods, employing computational design to simulate the deployment of structural lattices based on auxetic and kirigami patterns. These methods demonstrate how design intent can inform the pattern generation process, allowing designs to be produced that adapt to different requirements and use cases [7,9,10]. However, these methods are primarily developed for two-dimensional, CNC-fabricated sheet systems and do not address the structural and fabrication challenges associated with producing self-supporting structural systems at the architectural scale.

This paper addresses this gap by presenting a computational workflow for designing, fabricating and erecting freeform deployable structures based on auxetic lattice mechanisms, to advance the application of programmable metamaterials in architectural structures. The workflow translates a given target 3D geometry, representing an architectural design concept, into a kinematically compatible system and implements a form-finding procedure that integrates kinematic constraints and fabrication logic to produce structurally viable and fabrication-ready components. Beyond the production of digital models

and computational workflows, this work also includes materialization studies and preliminary physical tests, leading to full-scale mock-ups used to evaluate structural behavior, manufacturing constraints, and deployment performance.

3. Methodology

The computational design-to-fabrication workflow developed in this research, shown in Figure 1, is structured into three stages: form-finding (A), materialization (B), and prototyping (C). Form-finding (Figure 1-A) begins with the definition of a kinematic system and a target shape. Initial models for both the deployed and flat configurations are generated and evaluated simultaneously using a constraint-based form-finding solver. Geometric and kinematic relationships between corresponding elements in the flat and deployed configurations are enforced, resulting in a compliant geometry. Compliance is assessed through geometric accuracy and kinematic feasibility analyses. Materialization (Figure 1-B) involves running linear and non-linear structural analyses to inform material selection and component sizing. The design is iteratively refined through geometric optimization aimed at enhancing structural performance in the deployed state while ensuring fabrication efficiency in the flat state. The process concludes with the selection of a final solution and structural detailing, leading to the production of fabrication data for additive manufacturing processes. Prototyping (Figure 1-C) was carried out alongside digital simulations to further validate design solutions during and after the deployment process and inform the development of technical solutions to support assembly and erection processes for specific design needs. The main components of the workflow were developed through iterative feedback and validation loops to progressively address form-finding, materialization, and prototyping challenges. They are described in turn in the subsections below.

3.1. Form-finding

The first step of the workflow involves defining a kinematic system to control the deformation of a flat lattice and its deployment into a 3D shell structure (Figure 2). The kinematic system is implemented in Kangaroo 2 for Grasshopper (Rhinoceros 3D) to simulate the deployment of various lattice configurations through digital form-finding. The kinematic system is based on rotating polygon structures, which enable the controlled expansion or contraction of the flat lattice through cell rotation. This system does not require discrete hinges, making it well-suited for additive manufacturing.

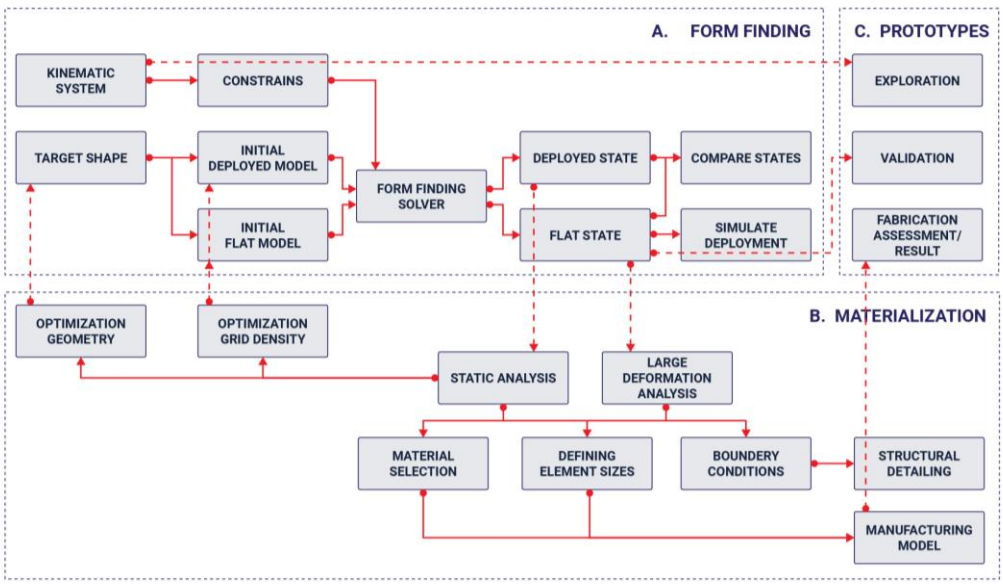

Figure 1: Workflow diagram including (A) form-finding, (B) materialization, and (C) prototyping stages. The workflow links flat and deployed configurations through constraint-based form-finding, followed by structural analysis, structural detailing, production of data for digital manufacturing, and validation/refinement through iterative prototyping

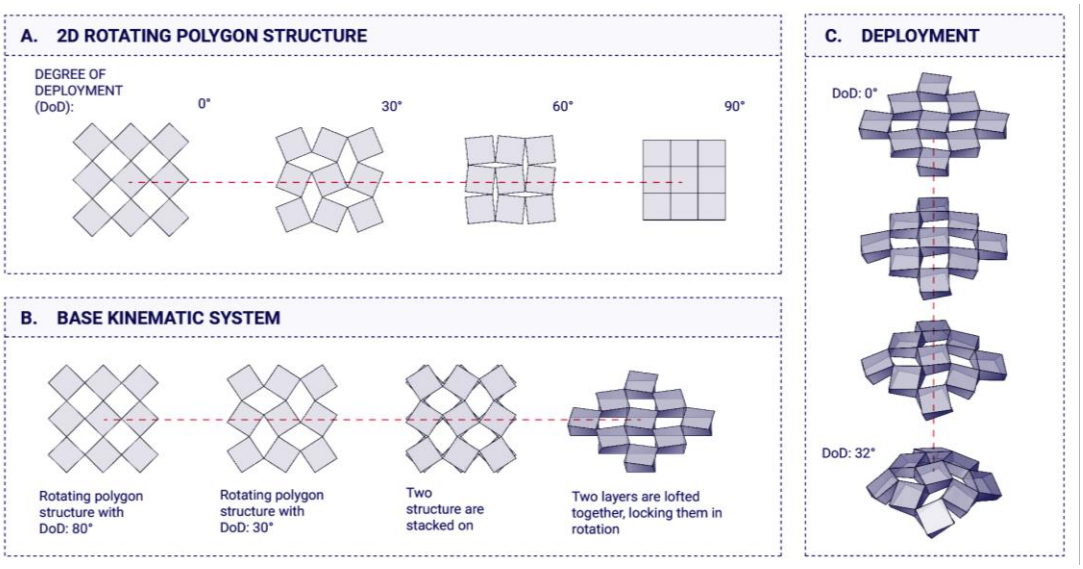

Figure 2: Definition of the kinematic system based on rotating polygon structures in three stages: (A) construction of a 2D grid of rotating square cells; (B) generation of a layered 3D cell structure through vertical stacking of 2D grids; (C) simulation of the deployment process.

Furthermore, its parametric definition allows curvature and deployment process to be controlled, enabling the generation of a wide range of geometries while maintaining fabrication compatibility. The kinematic system is defined in three stages (Figure 2). Stage A produces the 2D pattern as a grid of square cells connected at the vertices, forming an alternating pattern of rotating elements and void spaces that define the kinematic relationships within the system. The variable 'Degree of Deployment' (DoD) controls the system's contraction and expansion by affecting the relative positions of contiguous cells. Stage B produces 3D cells by stacking two 2D patterns of square cells with DoD values 30° and 80° along the z-axis by distance h (thereby generating a top and bottom layer) and lofting the edges of corresponding cells. Stage C simulates the deployment process by varying a global DoD parameter, generating a doubly curved 3D geometry (DoD = 32°) from an initially flat configuration (DoD = 0°).

3.1.1. Initial models

Figure 3 shows how the kinematic system adapts to different classes of shell geometries - synclastic, anticlastic and monoclastic surfaces - by creating two initial models: one for the target surface and one for the flat configuration. A diagonal mesh is generated on the target surface to define the deployed configuration. This mesh is then subdivided into a checkerboard pattern of alternating rotating polygons and void spaces, as described in Section 3.2.1, to establish the primary kinematic relationships within the system (Figure 3A). The same subdivision is applied to an offset mesh to produce the second layer, generating 3D cells through a lofting operation between corresponding rotating polygons on the two layers. The deployed mesh is then converted into a mass-spring system and relaxed into a planar configuration using the dynamic relaxation solver embedded in Kangaroo. Since geometric and kinematic discrepancies between the target and flat states are unavoidable during planarization, this planar configuration serves as an initial approximation of the flat state, which is subsequently corrected through the form-finding process described below.

3.1.2. Dynamic relaxation

A set of constraints is defined within the dynamic relaxation process to minimize the geometric differences between the two initial models, corresponding to the flat and deployed configurations. These constraints ensure a kinematically compliant transformation between the flat and deployed states. The constraint system is organized into four categories (Table 1), each addressing a specific aspect of geometric consistency.

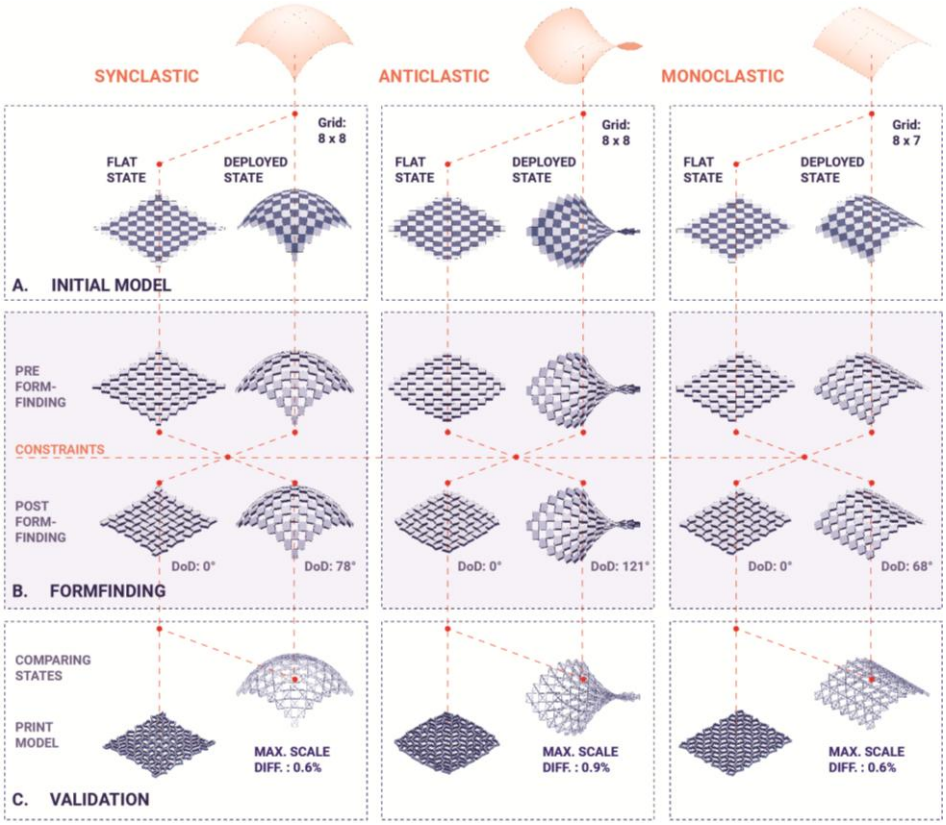

Figure 3: Form-finding process applied to synclastic, anticlastic, and monoclastic target geometries. (A) Initial model setup. (B) Form-finding input and resulting configurations. (C) Validation through comparison of flat and deployed states, and development of a prototype model.

The two initial models and the constraint system form the input for the dynamic relaxation solver in Kangaroo 2 (Figure 3B). The flat and deployed configurations are solved simultaneously by iteratively adjusting node positions. The goal is to minimize differences in corresponding element lengths between the two configurations while satisfying all constraints. Because internal dimensions are restricted by internal constraints and the global Equal Length Constraint, the elements of the flat state are allowed to rotate only to satisfy the state conditions (Figure 3B). This results in two closely related configurations. The Degree of Deployment (DoD) is defined as the average rotation of the polygon units required to achieve the deployed state. Different target geometries require different DoD values (synclastic ≈ 78°, monoclastic ≈ 68°, anticlastic ≈ 121°), indicating that anticlastic geometries are more difficult to approximate (Figure 3B).

3.1.3. Validation

The resulting geometries are assessed by comparing the element lengths of the flat and deployed configurations. Length variations are used to identify local distortions and guide adjustments to the target geometry, grid resolution, or constraint definition. Across the three target geometries, all configurations remain below 1% deviation, which is acceptable for flexible materials such as TPU. Scale differences are 0.6% for monoclastic and synclastic cases, and 0.9% for the anticlastic case. The higher deviation in the anticlastic configuration reflects increased strain due to its more pronounced curvature. Additional validation is performed using physical models as discussed in Section 3.3.

3.2. Materialization

The second step of the workflow, materialization (Figure 1B), involves translating the digital model produced through the form-finding process into a fabricable system, enabling the deployable structure

to be realized at the architectural scale. To evaluate this translation, the workflow was applied to the design of a small event shelter. Figure 4 visualizes the complete design-to-fabrication workflow applied to this case study. The following subsections focus on the materialization process, starting with the selection of material that meets the project requirements, moving to structural analysis and optimization, and detailing for final production and full-scale assembly.

Table 1: Constraint system used in form-finding, defining geometric, kinematic, and state conditions to ensure compatibility between flat and deployed configurations.

Category	Description	Function
Global Equal Length Constraint	Enforces identical lengths between corresponding elements in the flat and deployed states.	Couples both configurations and ensures kinematic compatibility during form-finding.
Internal Constraints	Preserve unit cell geometry by maintaining edge lengths, diagonals, and cantering, while allowing controlled deformation.	Maintains structural coherence of each cell while enabling relative rotation between layered polygons.
Kinematic Constraints	Define rotational relationships between neighbouring elements, applied within the void spaces of the system.	Enables controlled contraction in the flat state and prevents element collision during deployment.
State Constraints	Impose global conditions for each configuration, including flat-state planarity, deployed-state target geometry, and boundary conditions.	Ensures each state satisfies its functional and geometric requirements.

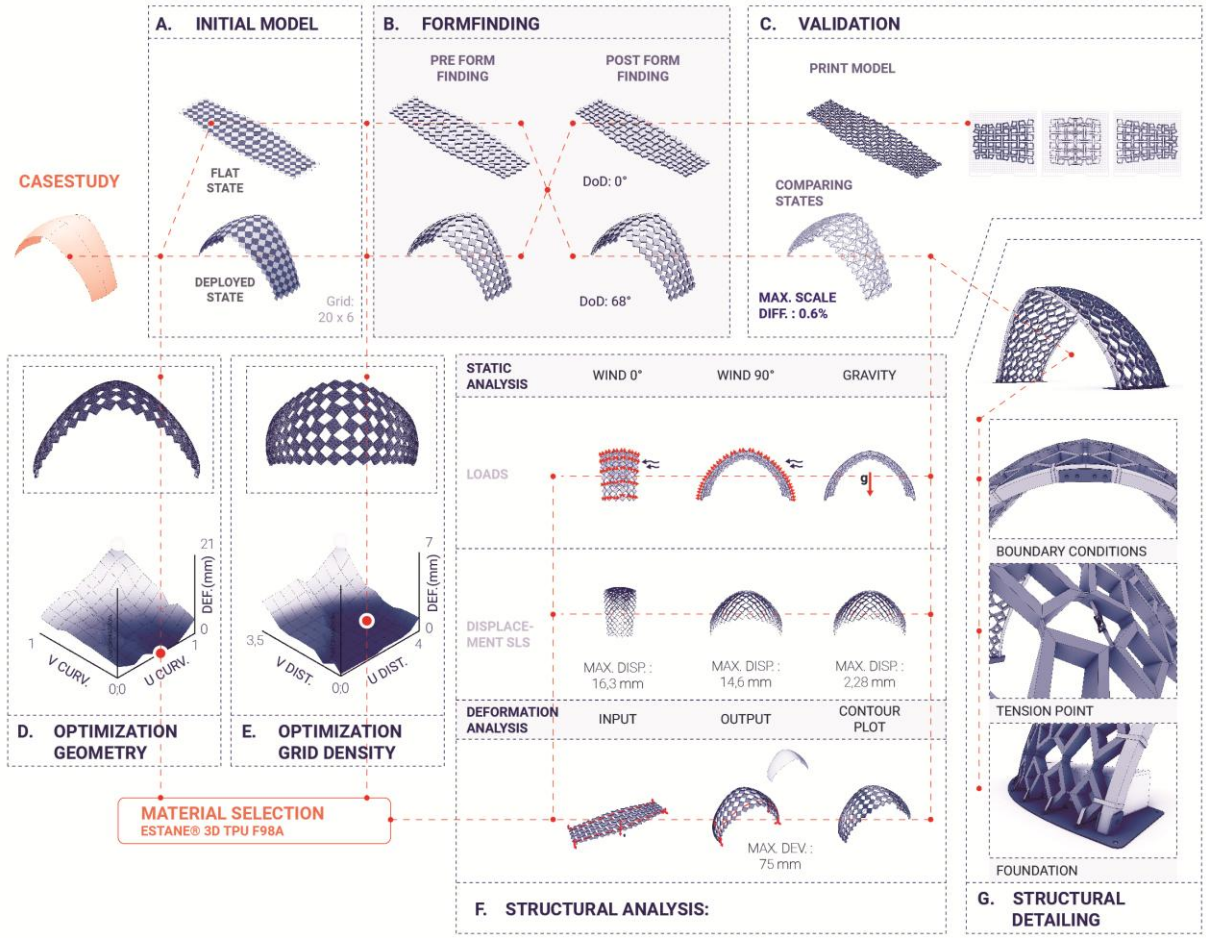

Figure 4: Complete computational design-to-fabrication workflow, including both form-finding and materialization stages, applied to a target event shelter design. (A–C) Overview of model setup, form-finding, and validation. (D–E) Optimization of global geometry and grid density. (F) Structural analysis under gravity and wind loads. (G) Structural detailing, including boundary conditions and tension-based actuation.

3.2.1. Material selection

Material selection was informed by the main project goal, which is to produce deployable structures through the additive manufacturing of large-scale components. Due to the current single-material limitation of most large-scale additive manufacturing systems, rigid elements and compliant joints had to be realized within a single material system. This introduced a trade-off between global rigidity and local hinge compliance, making material selection a critical design choice.

Consultations with industry partners BouwLab indicated that large-scale printing with flexible materials, such as TPU and TPE, remains uncommon due to limited demand and experience, resulting in a restricted range of suitable materials. BouwLab provided a selection of commercially available materials compatible with large-scale printing. From this selection, "ESTANE® 3D TPU F98A-030 CR HC PL" [11] was selected to prioritize structural stability, while hinge behavior was addressed through geometry. Due to limited available data, material properties for analysis were partially estimated based on TPU materials with comparable Shore hardness.

3.2.2. Structural analysis

Figure 4F illustrates the structural analysis conducted with Karamba3D, a finite element analysis plug-in operating within Grasshopper. The polygonal cells generated during the form-finding process are translated into shell elements by lofting corresponding cells between the top and bottom layers. Additional links between neighboring cells form the compliant hinges (Figure 4F). The structure is fixed along the ground edges. Two complementary analyses are performed: (1) a geometrically nonlinear analysis, implemented through the large deformation component in Karamba3D, which simulates deployment from the flat state, allowing hinge behavior and deviation from the target geometry to be monitored; and (2) a linear static analysis that evaluates the performance of the deployed configuration under operational loads.

The large deformation analysis (Figure 4F, bottom) simulates deployment by applying cable pretension loads. This step evaluates geometry only and excludes deployment stresses. The input model is constrained to allow in-plane motion only, and the resulting geometry is compared to the target design using distance maps. Multiple cable arrangements were tested, and a 10-point tension system was selected as a valid compromise between target design approximation and the number of tension points. This system produced geometries closely aligned with the target design, with maximum deviations of approximately 7.5 cm, primarily along the edges.

The linear static analysis (Figure 4F, top) assesses the deployed structure under simplified wind loads. Pinned supports are applied along the perimeter after initial ground-only supports resulted in excessive deformation under 90° wind loads. Loads follow Eurocode-based assumptions for Region II and consequence class CC1, with pressure on the windward side and suction on the leeward side. With full edge support and the selected material system, acceptable stress levels and deformations are achieved across all load cases, with a maximum displacement of 1.63 cm in the critical serviceability case.

3.2.3. Design optimization

The model is further refined through two grid-search processes, shown in Figure 4D–E, to (1) evaluate how geometric parameters influence structural performance and (2) identify parameter combinations that produce high-performing design solutions. Both studies include a fitness landscape plot in which the X- and Y-axes represent different parameter pairs, while the Z-axis visualizes the maximum deflection of the analyzed deployed structure.

The fitness landscape plot in Figure 4D analyses the effects of varying curvature in the U direction, corresponding to the short span, and the V direction, corresponding to the long span, on structural performance, with parameter values mapped onto the X- and Y-axes, respectively. The graph shows that lower curvature in the U direction generally reduces deformation, whereas increasing curvature along

the V direction leads to higher maximum displacement. The fitness landscape plot in Figure 4E explores the effect of mesh density on structural performance. Local mesh density is controlled through a Gaussian-based spacing function, parameterized by two variables controlling the Gaussian spread in the U and V directions. The plot shows that local adjustments produce consistent but modest reductions in maximum deflection of approximately 5% compared to the baseline uniform grid design. The best-performing configuration, highlighted in Figure 4E, is carried forward for further development.

3.2.4. Structural detailing and fabrication

Figure 4G illustrates structural details designed to turn the optimized geometry into a buildable system. These details are intended to ensure structural stability during and after deployment and to facilitate the deployment process. The design includes arched edge beams that are connected to the structure after deployment to provide lateral stiffness and distribute loads along the perimeter, as defined in Section 3.2.2. Tension points are integrated at ten locations across the undeployed structure, enabling controlled actuation through a ratcheting cable system and guiding the flat geometry into its target configuration. The structure is then either mechanically anchored to custom base plates or stabilized with ballast weights.

3.3. Prototyping

Physical prototyping is integrated throughout the workflow to evaluate geometric accuracy, joint behavior, and fabrication tolerances. Observed discrepancies between simulated and physical results were used to refine stiffness assumptions and fabrication parameters, establishing a feedback loop between design and realization. Figure 5 shows a selection of 3D-printed prototypes produced throughout the project. Figure 5A illustrates a series of small-scale models developed during the exploratory phase, which tested different types of TPU, print settings, and element dimensions (Figures 5B-D). Results from these tests identified TPU 92A combined with 0.8 mm compliant hinges and rigid elements of approximately 5 mm as a valid prototyping configuration. Figures 5B-C present models of synclastic and anticlastic shells printed in TPU 92A at various scales, which were used to validate the results of the form-finding process from a geometric point of view. Both models closely resemble their digital counterparts. However, the anticlastic shell model did not fully maintain its shape after deployment, indicating plastic deformation. This is likely caused by the larger degree of deployment (121°, Figure 3B) required to achieve the anticlastic curvature, which introduces higher strain in the compliant hinges and reduces geometric stability. Figure 5D shows a 1:10 scale model of the case study, printed in TPU 92A and subdivided into small components to simulate the production and assembly of the system at full scale. The geometry is segmented into modules whose maximum size is compatible with the printer's build volume, thus simulating production constraints. Figure 5E presents large-format printing tests conducted with BouwLab using ENSOFT SO-161-70A, a material selected to provide sufficient flexibility in the compliant hinges. The full-scale (1:1) prototype confirms the feasibility of printing compliant hinges but highlights the system’s strong sensitivity to hinge stiffness. Increasing hinge thickness improves functionality but also increases self-weight and reduces structural efficiency, highlighting a performance trade-off that should be addressed in future research.

4. Results

The computational workflow described in this paper was effectively used to design deployable structures that approximate a range of target geometries, including monoclastic, synclastic, and anticlastic surfaces. Measured scale differences remained below 1% across all test cases, with slightly higher deviations observed in the anticlastic design. Physical models produced at multiple scales validated the digital simulations, demonstrating consistent deployment behavior. The printed models achieved stable deployed configurations and maintained the intended kinematic behavior throughout the transformation process, therefore validating the custom-developed form-finding process. Preliminary structural analysis conducted on a shelter design used as a case study indicates that the deployed configuration performs adequately under the considered boundary conditions and material assumptions.

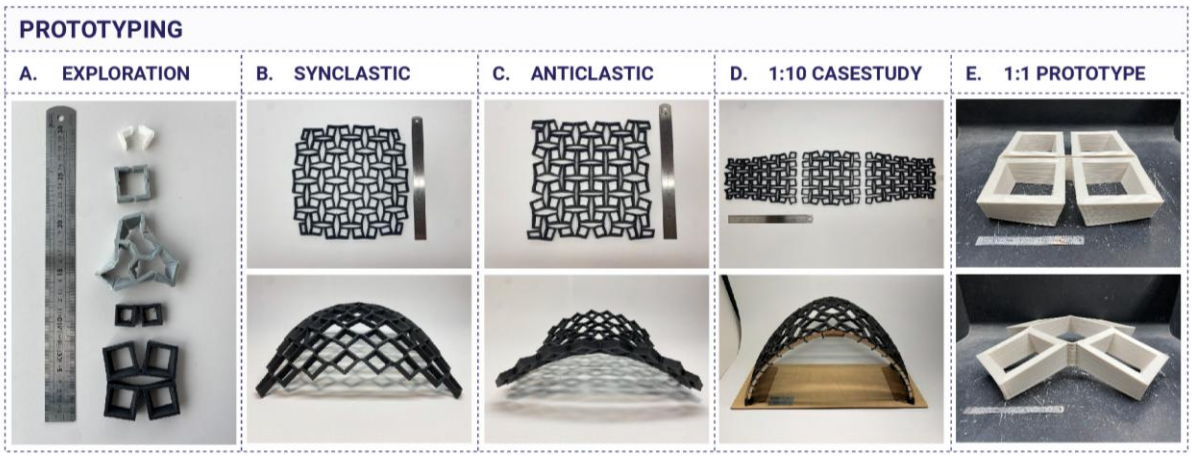

Figure 5: Prototyping iterations at various scales. (A) Exploration of the kinematic system and hinge fabrication in TPU; (B–C) small-scale validation of synclastic and anticlastic target geometries (TPU 92A); (D) 1:10 case-study model demonstrating the modular assembly strategy; (E) full-scale (1:1) printing of a deployable structural module with ENSOFT SO-161-70A.

The maximum unity check was found under ULS wind loading at 90°, reaching 82.1%, indicating that all elements remain within their design resistance. The maximum displacement was found under SLS wind loading at 0°, reaching 1.63 cm, which was considered acceptable relative to the overall structural span and serviceability requirements. Parametric studies further highlighted the effects of global geometry and local grid density on structural performance, providing a means to identify better-performing design solutions through grid-based search processes. Full-scale prototyping demonstrated the feasibility of manufacturing integrated compliant hinges using large-format additive manufacturing. The fabricated mock-up confirmed that 3D-printed hinges can effectively enable module deployment, providing initial data on the relationship between hinge geometry, material behavior, and deployment performance.

5. Discussion and conclusion

This paper presented a computational workflow for designing and fabricating deployable auxetic shell structures using additive manufacturing processes. The workflow integrates form-finding, structural evaluation, materialization, and prototyping to support the development of deployable structural systems at the architectural scale. In doing so, the research extends existing inverse design approaches to fabrication-aware architectural applications.

The first contribution of the study lies in the development of a constraint-based form-finding process capable of linking flat and deployed configurations, producing designs that consistently maintain kinematic compatibility across a variety of target geometries. The process can therefore be effectively used for designing deployable structures in which geometric transformation is embedded directly into the lattice organization rather than achieved through conventional mechanical assemblies.

A second contribution lies in the physical realization of the system through iterative prototyping and full-scale fabrication tests. While previous work on mechanical metamaterials and deployable systems has primarily focused on computational modelling or small-scale demonstrators, this research investigated the feasibility of producing such systems under architectural fabrication constraints, including print resolution, material limitations, hinge detailing, assembly logic, and self-weight effects. The prototypes demonstrate that compliant hinges can be integrated within additively manufactured structural components, while also revealing the sensitivity of the system to material stiffness and hinge geometry.

The study also identified several limitations that should be addressed in future research. Structural simulations currently rely on simplified material assumptions and do not fully capture nonlinear material behavior, anisotropy introduced by layer-based 3D printing, or long-term hinge fatigue. At full scale,

achieving sufficient hinge flexibility required increased local thickness, which improved manufacturability but introduced additional self-weight and reduced structural efficiency. These findings highlight the central design challenge of balancing global structural stiffness with local flexibility of compliant connections. Future development may address this through more advanced material characterization, multi-material additive manufacturing, or hybrid reinforcement strategies.

Despite these limitations, the presented workflow establishes a practical foundation for the design, fabrication, and deployment of lightweight programmable architectural structures. Compared with conventional deployable systems based on discrete hinges, scissor mechanisms, or articulated joints, the proposed approach reduces mechanical complexity by embedding deployment behavior directly into the printed geometry. This suggests potential applications in temporary shelters, event structures, adaptive roofs, and lightweight architectural enclosures where compact transport, rapid assembly, and geometric adaptability are required.

Acknowledgements

The authors would like to thank Bouwlab and 3DMZ for their support in material development and large-scale additive manufacturing, as well as the technical staff who supported the fabrication and testing of the prototypes described in the paper.

References

[1] S. Pellegrino, "Deployable structures in engineering," in *Deployable Structures*, S. Pellegrino, Ed. Vienna: Springer, 2001, pp. 1–35.

[2] G. E. Fenci and N. G. Currie, "Deployable structures classification: A review," *International Journal of Space Structures*, vol. 32, no. 2, pp. 112–130, 2017.

[3] J. Ou, Z. Ma, J. Peters, S. Dai, N. Vlavianos, and H. Ishii, "KinetiX: Designing auxetic-inspired deformable material structures," Computers & Graphics, vol. 75, pp. 72–81, 2018.

[4] A. Ion, D. Lindlbauer, P. Herholz, M. Alexa, and P. Baudisch, "Understanding metamaterial mechanisms," in Proceedings of the 2019 CHI Conference on Human Factors in Computing Systems, 2019, pp. 1–14.

[5] A. A. Zadpoor, "Mechanical metamaterials," Materials Horizons, vol. 3, no. 5, pp. 371–381, 2016.

[6] J. Panetta, F. Isvoranu, T. Chen, E. Siéfert, B. Roman, and M. Pauly, "Computational inverse design of surface-based inflatables," ACM Transactions on Graphics, vol. 40, no. 4, pp. 1–14, 2021.

[7] T. Chen, J. Panetta, M. Schnaubelt and M. Pauly, "Bistable auxetic surface structures," *ACM Transactions on Graphics*, vol. 40, no. 4, pp. 1–9, 2021.

[8] J. Pan, X. Li, Q. Zhang, S.-D. Kim, and J. Cai, "Chiral multi-stable kirigami metamaterials," in Proceedings of the IASS Annual Symposium 2025: The Living Past as a Source of Innovation, México City, Mexico, Oct. 27–31, 2025.

[9] M. Konaković-Luković, J. Panetta, K. Crane and M. Pauly, "Rapid deployment of curved surfaces via programmable auxetics," *ACM Transactions on Graphics*, vol. 37, no. 4, pp. 1–13, 2018.

[10] M. Konaković-Luković, J. Panetta, K. Crane, and M. Pauly, "Rapid deployment of curved surfaces via programmable auxetics," ACM Transactions on Graphics, vol. 37, no. 4, pp. 1–13, 2018.

[11] Lubrizol Corporation, "ESTANE® 3D TPU (Thermoplastic Polyurethane)," Available: https://www.lubrizol.com/solutions/products/estane/estane-3d. Accessed: May 17, 2025.

[12] Karamba3D, "Karamba3D: Parametric engineering tool." [Online]. Available: https://www.karamba3d.com/. Accessed: May 17, 2025.